Light Metals 2012 *Edited by: Carlos E. Suarez*
TMS (The Minerals, Metals & Materials Society), 2012

WETTING OF KF-ALF$_3$-BASED MELTS ON GRAPHITE CATHODE MATERIALS FOR ALUMINUM ELECTROLYSIS

Yanan Zhang, Jilai Xue, Jun Zhu, Xiang Li
School of Metallurgical and Ecological Engineering, University of Science and Technology Beijing;
Xueyuan Road 30; Beijing 100083, China

Keywords: Wetting, KF-AlF$_3$-based Melt, Graphite Cathode Materials, Ultrasound

Abstract

Graphite cathode materials are nowadays used in aluminum reduction process where KF-AlF$_3$-based melts may serve as an alternative electrolyte. In this work, wetting angles of KF-AlF$_3$-based melts on graphite cathode materials were measured using a modified sessile drop method. A fresh drop of the melt was injected through a BN tube on to the samples surface, and then the wetting angles were photographed against time elapsed. It was found that the wetting angles on the full graphitic and graphitized cathode samples were larger than those on the semi-graphitic at 750 °C, and their values changed with varying alumina content (3-5 wt%), cryolite ratio (1.2-1.5) and time (0-20 min). The melt penetration profiles on the cross-sections of the melt-graphite interface after wetting tests were also inspected using SEM-EDS technique. In addition, ultrasound was introduced into the cathode through a stainless steel rod and its effect on the wetting of melts was investigated.

Introduction

Aluminum metal is produced in Hall-Heroult reduction process where graphite cathode materials are widely used nowadays. In recent years, low-temperature aluminum electrolysis has been developed to improve electrical energy efficiency. It has been found that the current efficiency will in general increase about 1 - 2 % for each 10 °C decrease in electrolyte [1]. In the cryolite systems used for low temperature aluminum electrolysis, KF-AlF$_3$-based melt has been considered as potential electrolyte due to its lower eutectic temperature and higher alumina solubility [2-5]. Their physical and chemical properties, such as melting temperature, alumina solubility, electrical conductivity, etc. can be found in open literature [2-8].

Furthermore, the service life of aluminum reduction cells is strongly affected by the melts penetration into cathodes, carbide formation and dissolution, while the penetration process is in correlation with the wetting of cryolite on the cathodes. Liu et al. [9] had investigated the wettability of sodium cryolite-alumina melts on varying graphite content cathode blocks, where the wetting angles of cryolite-alumina melts on the cathodes with various graphite contents decreased with testing time. Anton V et al. [10] found that the wetting of the melts {[93.5 % (NaF-AlF$_3$)$_{CR=2.3}$ + 6% CaF$_2$ + 0.5% MgF$_2$] + 5% Al$_2$O$_3$} on different materials had improved with increased cathode current density, and then the melts penetration depth after wetting was dependent on the open porosity of the cathode materials. It is, however, scarce in open literature to find information on the wettability of KF-AlF$_3$-based melts on graphite cathode materials.

In this work, the wettability of KF-AlF$_3$-based cryolite on industrial graphite cathodes was investigated using a modified sessile drop method. Contact wetting angles were measured against time during the test at 750 °C, which changed with varying alumina content and cryolite ratio. The cross-section of the melt-graphite interface after wetting-penetration tests were inspected by SEM-EDS technique. In addition, the effect of ultrasound on the wetting process of KF-AlF$_3$-based melts on graphitized cathode was also studied for potential use of this technology in improving energy efficiency during aluminum electrolysis [11].

Experimental

Materials and Chemicals

The cathode samples in cylindrical form used in this work were directly taken from the industrial cathode blocks of semi-graphitic (HC35), full graphitic (HC100), and graphitized cathodes (SMH). The samples were sliced along their horizontal axis for about 5 mm thick each, and then were polished mechanically in several steps to minimize the influence of roughness on the wettability of the cathode samples.

Table I lists the statistical data on the properties of pores in the cathode samples, which was obtained previously by image analysis [12]. Table II presents the compositions of the melts used in this investigation. All the chemicals were analytical grade with purity ≥ 98 *wt.*%, which were premelted to form the electrolyte in argon atmosphere before test.

Table I. Statistical Data about Pores in Cathode Samples

Samples	Pores numbers	Average Diameter of Pores (μm)	Specific Surface Area of Pores (μm^2/μm^3)	Connectivity (%)
HC35	230	186.61	0.017	54.2
HC100	488	135.97	0.029	28.1
SMH	438	182.31	0.023	48.7

Table II. Composition of the Melts Used in Experiments

Melts	CR	*wt.*%Al$_2$O$_3$
KF (44.40%)-AlF$_3$ (52.60%)	1.22	3.0
KF (43.48%)-AlF$_3$ (51.52%)	1.22	5.0
KF (44.98%)-AlF$_3$ (50.02%)	1.30	5.0
KF (48.39%)-AlF$_3$ (46.61%)	1.50	5.0

Sessile Drop Method

Figure 1 shows the experimental set-up for modified sessile drop method that was used to measure the contact wetting angles of cryolite melts on the cathode materials. In order to assure a drop of the melts exactly down in contact with the solid samples, the mass of the cryolite was all 0.24 g for each experiment. And the electrolyte was put into a BN tube having a Φ0.5 mm needle hole at the bottom end. Then, the BN tube was set into the furnace that was sealed and vacuumed.

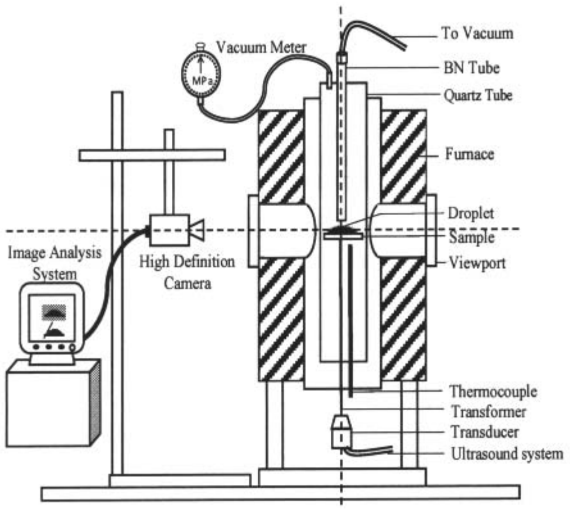

Figure 1. Schematic drawing of experimental set-up for sessile drop method.

During experiments, the furnace was first heated up to the test temperature. After about 5 minutes, the cryolite in the BN tube was melted and dropped through the needle hole, down to the sample surface. The real-time contact wetting angles were recorded by a high-definition digital camera (MVC-II-1M), and the curve of contact wetting angle *vs*. time was obtained. After the wetting test, the cathode samples were cut out along the direction of perpendicular to the wetted surface, and the information of the melt penetration was inspected using SEM-EDS technique.

Ultrasound device was placed at position under the furnace. The ultrasound transducer was connected with a stainless steel rod that was mounted to SMH cathode sample. The sonic waves were transferred through the stainless steel rod onto the interface of the cathode sample and the melt drop. The ultrasound frequency was 20 kHz, and the power of ultrasound was 180 W with ultrasound-on for 2 seconds and -off for another 2 seconds, alternatively.

Data Processing

In Figure 2, the scheme drawing illustrates the calculating procedure of the wetting angle from the shape of the drop using Image J software (a public domain, Java-based image processing program developed at the National Institute of Health). The obtained photos about the wetting were processed using this software to enhance the image quality and then calculate the wetting contact angles. The software was employed to define the contour of the drop as a B-spline curve, which was extended by mirror symmetry to determine the interfacial contact points. And the contact angle was an average of the contact angles on both sides of the drop, $\angle\theta_1$ and $\angle\theta_2$.

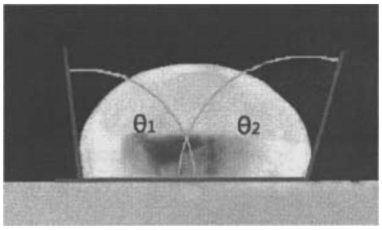

Figure 2. Scheme drawing of wetting angle calculation.

Results and Discussion

Effect of the Graphitization Degree

Figure 3 is the photographs showing the wetting process of the melt drops against testing time elapsed on various cathode samples at 750 °C. The contact angle of each drop was then calculated using the image analysis technique. All the drops here were made of KF-AlF_3 (3 wt.% Al_2O_3, CR=1.22), and their wetting behaviors were found having a similar tendency on HC100 and SMH cathode samples with a poorer wettability than that of HC35.

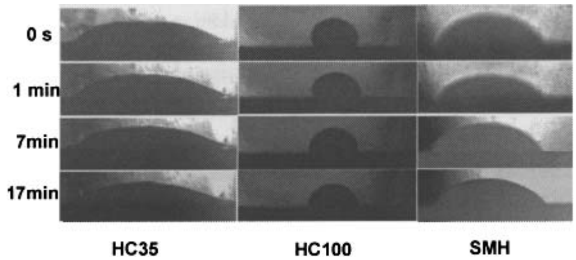

Figure 3. Photographs of KF-AlF_3 melts (3 wt.% Al_2O_3, CR=1.22) wetting on the three cathode samples at 750 °C

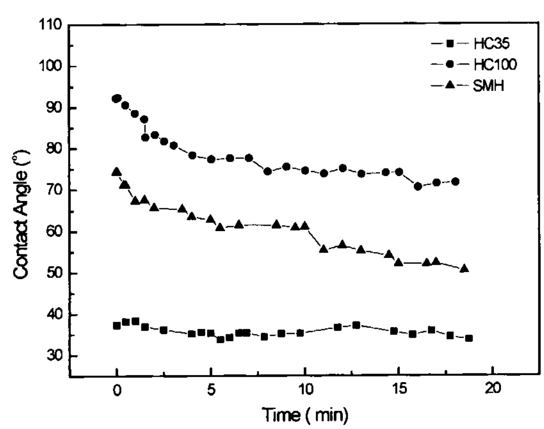

Figure 4. Curves of contact angles vs. time during wetting process of KF-AlF_3 melts (3 wt.% Al_2O_3, CR=1.22) on graphitic and graphite cathodes at 750 °C.

Figure 4 shows the curves of the contact angles *vs*. time during wetting process of KF-AlF_3 melts (3 *wt*.% Al_2O_3, CR=1.22) at 750 °C, which were obtained from the photographs similar to Figure 3.

Furthermore, Table III gives some special contact angles on these curves. The initial contact angles are the ones that have established just at the moment the melt drop is forming a stable shape on the cathode samples, which show their values in the order of HC100 > SMH > HC35; the equilibrium contact angles are the ones that have showed at the moment the drop is spreading to a shape unchanged for a relative long period, which have the tendency similar to the order for the three cathode samples. These facts means that the wettability of $KF\text{-}AlF_3$ melt on the three cathode materials tested have a general order as HC100 < SMH < HC35. The change between the initial to the equilibrium contact angles, $\Delta\theta = \theta_1 - \theta_2$, is very small for HC35, while they are relative large for both HC100 and SMH cathode samples. These imply that the wetting process may be affected by the variation in graphitized degree among the three cathodes. .

Table III. Details of Contact Angles from Curves in Figure 4

Sample	Initial contact angles, θ_1	Equilibrium contact angles, θ_2	$\Delta\theta = \theta_1 - \theta_2$
HC35	37°	35°	2°
HC100	92°	74°	18°
SMH	74°	61°	13°

Effect of Al_2O_3 Content and Cryolite Ratio (CR)

Figure 5 shows that the contact angles of the $KF\text{-}AlF_3$ melt with 5 *wt.*% Al_2O_3 were larger than those with 3 *wt.*% Al_2O_3 (both CR = 1.22) at 750 °C on SMH cathode samples. This means that the wettability of the $KF\text{-}AlF_3$-based melts on SMH cathode material could be worse with an increased Al_2O_3 content in the system. Moreover, the contact angles after reaching the equilibrium (about 11 min later) can be further lower until a stable value in the range of testing time. Such a similar phenomenon was also reported somewhere else with explanation that the volatilizations of the tested melt and the absorption of cathode material might be the cause for reducing the wetting contact angle [13].

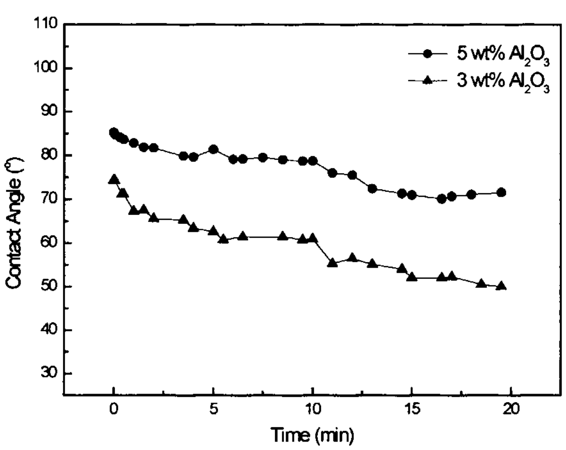

Figure 5. Curves of contact angles vs. time for different Al_2O_3 contents in $KF\text{-}AlF_3$ melts wetting on SMH cathode material at 750 °C (CR = 1.22).

The contact angles of $KF\text{-}AlF_3$ melt *vs.* time, as shown in Figure 6, change with varying CR value on the same SMH cathode material at 750 °C. A higher value of CR in $KF\text{-}AlF_3$ melts can improve its wettability. Similar phenomenon that the surface tension of sodium cryolite melts decreases with an increased CR value, has been reported [14], which might suggest a mechanism for the potassium cryolite melt to reduce its wetting contact angle on the graphite cathode materials.

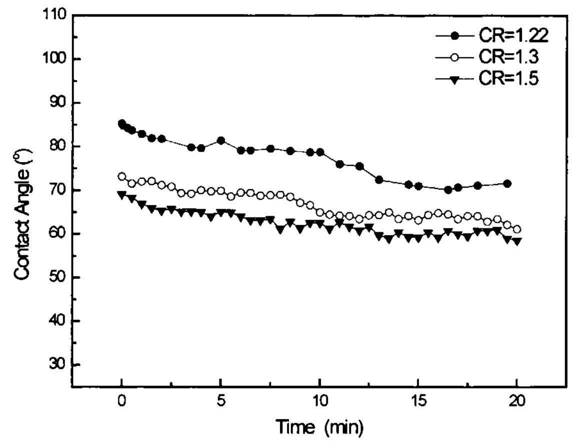

Figure 6. Curves of contact angles vs. time during wetting of $KF\text{-}AlF_3$ melts with various CR (5 wt.% Al_2O_3) on SMH cathode material at 750 °C

Effect of Ultrasound

Figure 7 demonstrates that the effects of ultrasound on the wetting process of $KF\text{-}AlF_3$ melts on SMH samples at 750 °C. The ultrasound wave was operated at 750 °C with interval of on and off, alternatively. The contact wetting angles with ultrasound are all larger than those without ultrasound.

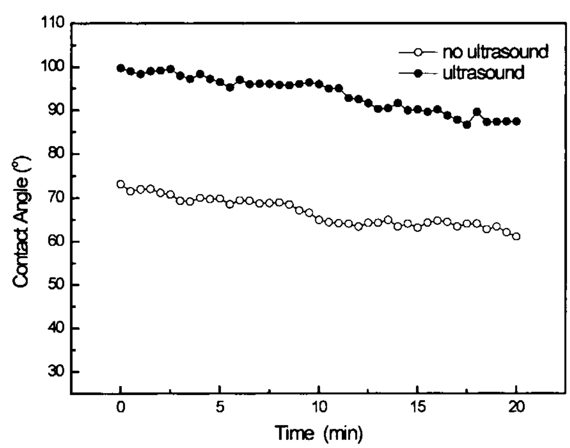

Figure 7. Curves of contact angles vs. time during wetting process of $KF\text{-}AlF_3$ melts (5 wt.% Al_2O_3, CR=1.3) on SMH cathode samples with ultrasound at 750 °C

Table IV shows that when ultrasound is applied, the initial (θ_1) and equilibrium contact angles (θ_2) of the melt become larger, but the variation ($\Delta\theta$) with time is roughly equal. Compared with no ultrasound, the time of reaching equilibrium was extended from 3 min to 5 min with ultrasound-on, while the time of keeping equilibrium was increased from 3.5 min to 6 min. This means that the ultrasound could reduce the wettability of the melts on SMH cathode material, and slow down the speed of the electrolyte drop spreading on the cathode surface.

Table IV. Details of Contact Angles from Curves in Figure 7

Operation	Initial contact angles, θ_1	Equilibrium contact angles, θ_2	$\Delta\theta = \theta_1 - \theta_2$
Ultrasound-off	73°	70°	3°
Ultrasound-on	100°	96°	4°

Wetting and Penetration of Potassium Cryolite Melts

Figure 8 presents SEM image and EDS-mappings of Al, K, and F at the melt-graphite interface after potassium cryolite melt (5 *wt.* % Al_2O_3, CR=1.5) wetting on SMH cathode material at 750 °C. It indicates that the penetrated melts were mainly located in the pores and micro-cracks, suggesting that the melt penetration might occur within these defected areas.

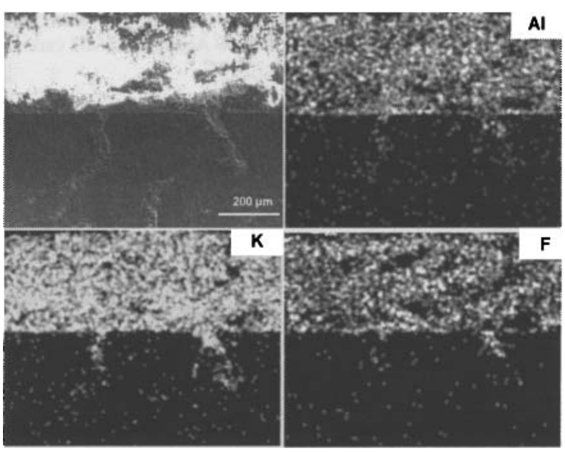

Figure 8. SEM image and EDS analysis on cross-sections at the melt-graphite interface after wetting tests (5 wt. % Al_2O_3, CR=1.5) on SMH cathode material at 750 °C

Table V. SEM-EDS Analysis of Penetrated Melts within the Areas near the Melt-Graphite Interface of SMH Cathode Materials after Wetting Tests at 750 °C

Melts	Penetrated element content in the areas of 2.2 mm from the interface		
	K (%)	F (%)	Al (%)
$KF\text{-}AlF_3(CR{=}1.22)\text{-}Al_2O_3$ (3 *wt.*%)	0.51	0.89	0.34
$KF\text{-}AlF_3(CR{=}1.22)\text{-}Al_2O_3$ (5 *wt.*%)	0.29	0.67	0.21

Table V shows the percentage of K, Al and F from the penetrated melts within the areas near the melt-graphite interface of SMH cathode material. It was found that a poorer wetting (larger wetting contact angle) with a higher Al_2O_3 content (5 %) was appeared with a lower contents of penetrated K, Al and F within the cathode material. This fact suggests that reducing wettability of the melt on the graphite cathode materials could effectively decrease the melt penetration into the cathode materials. Similarly, the relationship of the wettability of the sodium cryolite melt with its penetration into the graphite cathode material can be found in the literature [10].

Conclusions

1. Wetting of $KF\text{-}AlF_3$-based melts on graphite cathode materials were measured using a modified sessile drop method. It is found that the wettability of potassium cryolite on the three cathode samples tested is in an order of HC35>SMH>HC100 at 750 °C.

2. The wettability on graphite cathode material increases with decreased Al_2O_3 content and increased cryolite ratio (CR) in the $KF\text{-}AlF_3$-based melts.

3. At 750 °C, when ultrasound is applied on the SMH cathode, the wettability of potassium melts on the cathode is reduced.

4. SEM-EDS analysis shows that the melt penetration occurs crossing the interface of melt-graphite after the wetting, where more melts penetration is associated with better wettability of $KF\text{-}AlF_3$-based melts on the graphite cathode material.

Acknowledgement

Part of work has been supported by National Natural Science Foundation of China (No. 50874012).

References

1. J. Evans, and H. Kvande, "Sustainability, Climate Change, and Greenhouse Gas Emissions Reduction: Responsibility, Key Challenges, and Opportunities for the Aluminum Industry", *JOM*, 60 (8) (2008), 25-31.

2. E. Robert et al., "Structure and Thermodynamics of Alkali Fluoride-Aluminum Fluoride-Alumina Melts. Vapor Pressure, Solubility, and Raman Spectroscopic Studies", *The Journal of Physical Chemistry B*, 101(1997), 9447-9457.

3. J. Yang et al., "Alumina Solubility in $KF\text{-}AlF_3$-based Low-Temperature Electrolyte System", *Light Metals 2007*, 2007, 537-541.

4. A. Apisarov et al., "A Liquidus Temperature of Cryolite Melts with Low Cryolite Ratio", *Metallurgical and materials transactions B*, 42B (2011), 236-242.

5. Y. Zaikov et al., "Electrolysis of Aluminum in the Low Melting Electrolytes Based on Potassium Cryolite", *Light Metals 2008*, 2008, 505-508.

6. E. Frazer, and J. Thonstad, "Alumina Solubility and Diffusion Coefficient of the Dissolved Alumina Species in

Low-Temperature Fluoride Electrolytes", *Metallurgical and materials transactions B*, 41B (2010), 543-548.

7. J. Hives, and J. Thonstad, "Electrical Conductivity of Low-Melting Electrolytes for Aluminum Smelting", *Electrochimica Acta*, 49(28) (2004), 5111-5114.

8. A. Dedyukhin et al., "Influence of CaF_2 on the Properties of the Low-Temperature Electrolyte", *Light Metals 2008*, 2008, 509-511.

9. S. Liu et al., "Study on the Wettability of Electrolyte for Graphite Cathode Blocks", *China Nonferrous Metallurgy*, 6(2008), 20-22 (In Chinese).

10. A.V. Frolov et al., "Wetting and Cryolite Bath Penetration in Graphitized Cathode Materials", *Light Metals 2006*, 2006, 645-649.

11. J. Xue, and H.A. Oye, "Bubble Behavior-Cell Voltage Oscillation during Aluminum Electrolysis and the Effects of Sound and Ultrasound", *Light Metals 1995*, 1995, 265-271.

12. Y. Gao, J. Xue, and J. Zhu, "Characterization of Sodium and Fluorides Penetration into Carbon Cathodes by Image Analysis and SEM-EDS Techniques", *Light Metals 2011*, 2011, 1103-1107.

13. K. Grjotheim et al., *Aluminium Electrolysis: the Chemistry of the Hall-Héroult Process* (Düseldorf: Aluminium-Verlag 1977), 147.

14. E. Dewing, and P. Desclaux, "The Interfacial Tension between Aluminum and Cryolite Melts Saturated with Alumina", *Metallurgical Transactions B*, 8B (4) (1977), 555-561.